

Transition Prediction Models - Literature Review

Shlomy Shitrit and Eran Arad

January 7, 2015

Abstract

The transition of a boundary layer from laminar to turbulent impacts the characteristics of a flow field, but its underlying physics has yet to be well understood. This literature review aims to give an overview of the more widely used approaches to model transition in Computational Fluid Dynamics (CFD). Several different methods are reviewed: the linear stability analysis method, the low Reynolds number turbulent closure approach, the correlation-based methods, the intermittency transport method and the laminar fluctuation energy method. The approaches are compared to one another, highlighting their respective advantages and drawbacks.

0.1 Transition Simulation - background

Laminar flow can be predicted by the linearized stability theory at finite Reynolds number. It does not predict turbulence. The initial breakdown of the flow through amplification of infinitesimal disturbances is followed by a complicated sequence of spatial changes. The end result is an unsteady and disorderly phenomenon known as turbulence. The whole process of change from laminar to turbulent flow is termed transition. It affects strongly the distributions of wall shear stress and surface heat transfer. The main reason of its complexity is that besides the simultaneous presence of laminar and turbulent flow, there is also the interaction between the two phases. The CFD tools used for flow prediction in the industry are mainly RANS solvers. In general, this kind of solvers does not feature any specific transition simulation capability. They only use turbulence models to estimate the Reynolds stress tensor in the whole computational domain. There are several reasons for this situation. Firstly, the transition process involves a wide range of scales and it is very sensitive to physical flow features such as pressure gradient or free stream turbulence level. Secondly, transition occurs through different mechanisms such as natural transition and bypass transition. The third complication is that the RANS averaging eliminates the effects of linear

In recent years, several attempts to include laminar-turbulent transition prediction within RANS computations have been carried out. They can be classified into three approaches. A first approach is to use low Reynolds number turbulence models [1] or special transition models [2]. Although it is a very natural way to implement transition prediction capabilities into RANS solver, this approach cannot model various phenomena related to transition. The use of low Reynolds number RANS models has proven unreliable in predicting the change in skin friction and heat transfer within the transition region. No model of this type performs satisfactorily under the influence of free stream turbulence intensity and pressure gradients. It is difficult to obtain the correct location of the onset of transition with this class of models.

A second approach, recently proposed by Langtry and Menter [3], consists in using transport equation models for the intermittency and some special variables that tracks transition (momentum thickness number). The solution of these equations defines the laminar and turbulent regions. It mimics the effects of transition without modeling its internal physics. The implementation of such method in RANS solver is natural and applies to any kind of mesh and geometry.

The third approach involves the use of a transition prediction method inside a RANS code. The goal is to compute the transition location within the RANS calculation, and to control the turbulence by means of the effective viscosity $\mu_{eff} = \mu + \Gamma\mu_t$, where μ is the laminar dynamic viscosity, μ_t is the turbulent eddy viscosity and Γ is an intermittency function. In the laminar region $\Gamma = 0$ and at the detected transition region Γ should rise to simulate the start of turbulence. A requirement for the transition detection method is a low computational cost which does not advocate for full linear stability analysis as well as Parabolized Stability Equations (PSE) methods in complex configurations. In this context two ways have been explored. The first way consists in using transition criteria to predict the occurrence of either TS waves or Cross-Flow (CF) transition. Computing the transition location can be carried out using either local or non local criterion. A criterion is local if it only uses information coming from cells where the criterion is applied. The second way consists in using the e^N methods, based on linear stability theory, to detect transition. The velocity profiles in the boundary layer, required to perform that stability analysis, can then be obtained in two manners. The first one is to extract the velocity data directly from the RANS mesh, but this method has been shown to require a high grid resolution in the boundary layer. The other procedure to obtain a high resolution velocity profiles is by solving the boundary layer equations. The input data for the boundary layer equations may be the RANS surface pressure.

Up to date, the most reliable predictions for 3D flows could only be obtained with methods that implemented inside the RANS code, because it is the only one able to model the main natural transition mechanisms, namely TS and CF instabilities.

0.1.1 Development of vorticity and the final transition

The theory predicts that the initial instability occurs as two dimensional Tollmien-Schlichting waves, traveling in the mean flow direction. Three dimensionality soon appears as span wise

variations in velocity and pressure. The stretched vortices break into smaller units and local changes occur at random times and locations in the shear layer [4].

The transition process in quiet boundary-layer flow past a smooth surface consists of the following processes:

1. Stable laminar flow.
2. Unstable two-dimensional Tollmien-Schlichting waves.
3. Development of three-dimensional unstable waves.
4. Vortex breakdown at region of high shear stresses.
5. Vortex breakdown into fully three-dimensional fluctuations.
6. Formation of turbulent spots.
7. Fully turbulent flow.

The phenomena are sketched as a flat plate flow in figure 0.1.1 [4].

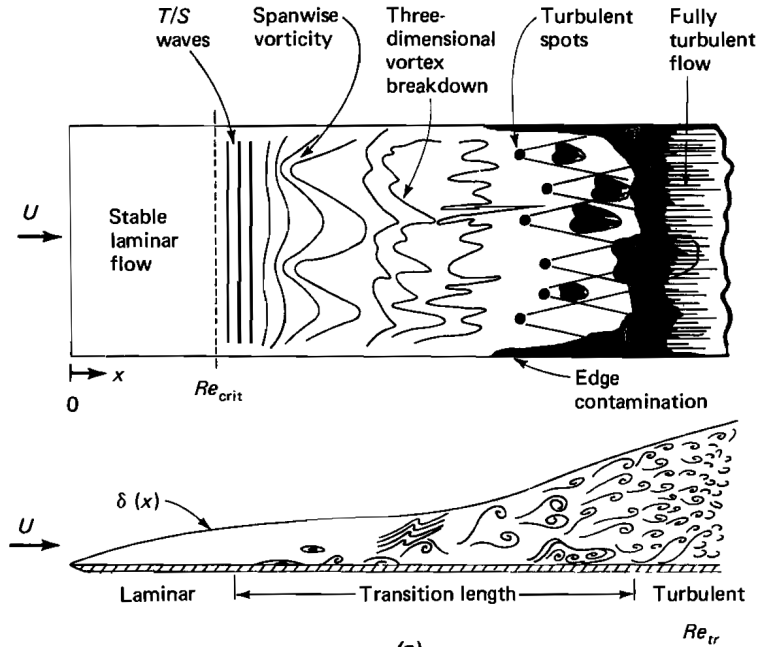


Figure 0.1.1: Description of the boundary layer transition process.

0.2 Definitions

This chapter is devoted to some definitions and provide data to assist in studies of viscous external flows. For the definitions below consider a uniform flow with velocity U moved parallel to a sharp flat plate of length L , as shown in Figure 0.2.2.

1. Boundary layer thickness δ - is the points where the velocity u parallel to the plate reaches 99 percent of the external velocity U . The accepted formulas for flat plate flow are:

$$\frac{\delta}{x} = \frac{5.0}{\sqrt{Re_x}}, \text{ laminar}$$

$$\frac{\delta}{x} = \frac{0.16}{Re_x^{1/7}}, \text{ turbulent}$$

where Re_x is the local Reynolds number of the flow along the plate surface.

2. Momentum thickness θ - is a measure of the total plate drag, and it also represents the length that has to be added on top of an airfoil to obtain the same total momentum as for an inviscid flow.

$$\theta = \int_0^{\delta} \frac{u}{U} \left(1 - \frac{u}{U}\right) dy.$$

3. **Displacement thickness** - An effect of a small displacement of the outer streamlines of a boundary layer, as shown in Fig. 0.2.2. The outer streamlines deflect outward a distance $\delta^*(x)$ to satisfy conservation of mass between the inlet and outlet

$$\int_0^h \rho U b dy = \int_0^{\delta} \rho u b dy, \quad \delta = h + \delta^*.$$

The quantity δ^* is called the displacement thickness of the boundary layer. The relation of δ^* to $u(y)$ is:

$$\delta^* = \int_0^{\delta} \left(1 - \frac{u}{U}\right) dy.$$

The displacement thickness is a measure for the thickness that has to be added on top of an airfoil if the solution would be computed inviscid.

4. **Critical Reynolds number** - For any given laminar flow, there is a finite value of its Reynolds number which cause the flow to become turbulent.
5. **Thwaite method** - Laminar and turbulent theories can be developed from Karman's general two dimensional boundary layer integral relation ,

$$\frac{\tau_w}{\rho U^2} = \frac{1}{2} C_f = \frac{d\theta}{dx} + (2 + H) \frac{\theta}{U} \frac{dU}{dx} \quad (0.2.1)$$

where $\theta(x)$ is the momentum thickness and $H(x) = \delta^*(x)/\theta(x)$ is the shape factor. This equation can be integrated to determine $\theta(x)$ for a given $U(x)$ if we correlate C_f and H with the momentum thickness. An example, taken from [4] of typical velocity profiles of laminar and turbulent boundary layer flows for various pressure gradients is shown in figure 0.2.1.

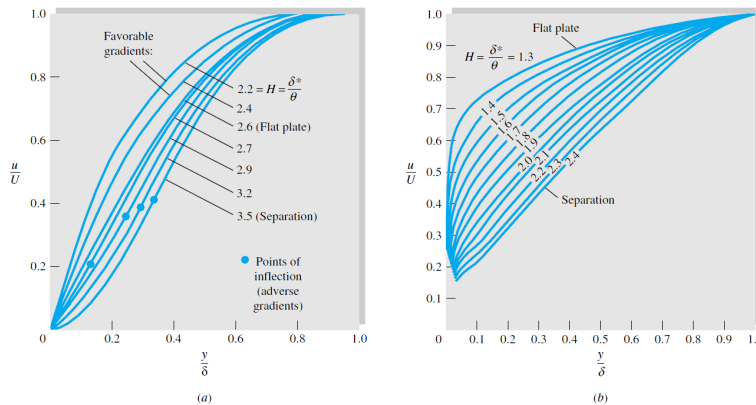


Figure 0.2.1: Velocity profiles with pressure gradients. a. laminar. b. turbulent

From this figure one can see that the shape factor H is a good indication of the pressure gradient, and separation occurs approximately at $H \approx 3.5$ for laminar flow and $H \approx 2.4$ for turbulent flow. For laminar flow a simple and effective method for the separation prediction was developed by Thwaites [5] who found that Eq. 0.2.1 can be correlated by a single dimensionless momentum thickness variable λ , defined as

$$\lambda = \frac{\theta^2}{\nu} \frac{dU}{dx}.$$

Using a straight line fit to his correlation, Thwaites was able to integrate Eq. 0.2.1 in closed form

$$\theta^2 = \theta_0 \left(\frac{U_0}{U} \right)^6 + \frac{0.45\nu}{U^6} \int_0^x U^5 dx,$$

where θ_0 is the momentum thickness at $x = 0$. Separation ($C_f = 0$) was found to occur at a particular value of $\lambda = -0.09$. Thwaites correlated values of the dimensionless shear stress $S = \tau_w\theta/\mu U$ with λ , and his graphed result can be curve-fitted as follows:

$$S(\lambda) = \frac{\tau_w\theta}{\mu U} \approx (\lambda + 0.09)^{0.62}$$

This parameter is related to the skin friction by the identity $S = 1/2C_f Re_\theta$.

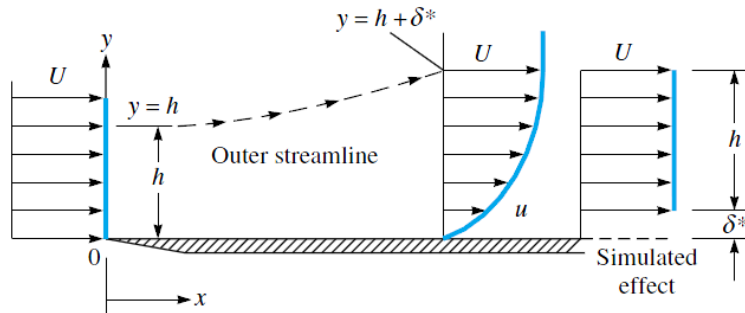


Figure 0.2.2: Displacement effect of a boundary layer.

0.3 Prediction of transition

Turbulence transition models have been broadly categorized in two groups:

1. models based on stability theory.
2. models not based on stability theory.
 - (a) models with specified transition onset.
 - (b) models with onset prediction capability.

0.3.1 Transition models based on linear stability analysis

The basic idea in linear stability analysis is to disturb a known mean flow with small perturbations. The mean flow is obtained by solving the boundary-layer equation. In the following, those disturbances will be represented by normal modes and the flow can be analyzed by solving an eigenvalue problem which shows if the disturbances are amplified or damped. In order to derive the equations which lead to the eigenvalue problem, the three-dimensional, incompressible continuity equation and Navier-Stokes equations are used [6]. In vector form those equations are written as follows:

$$\operatorname{div}(\vec{u}) = 0 \quad (0.3.1)$$

$$\frac{\partial \vec{u}}{\partial t} + \vec{u} \cdot \nabla \vec{u} = -\nabla p + \frac{1}{Re} \nabla^2 \vec{u} \quad (0.3.2)$$

where $u = \vec{U} + \vec{u}'$ is a composition of the mean flow \vec{U} found by solving the boundary-layer equations and the perturbation velocity \vec{u}' . Similarly, $p = p + p'$ is a composition of the mean pressure p and the perturbation pressure p' . In the most general approach the disturbances can have any form. Due to the fact that the mean flow fulfills the continuity equation and the Navier-Stokes equation those values can be subtracted from the mass and momentum equations. Further, the perturbations are assumed to be small and thus products of perturbation terms are neglected. Thereby, the linearized set of equations in vector form follows:

$$\operatorname{div}(\vec{u}') = 0$$

$$\frac{\partial \vec{u}'}{\partial t} + \vec{u}' \cdot \nabla \vec{U} + \vec{U} \cdot \nabla \vec{u}' = -\nabla p' + \frac{1}{Re} \nabla^2 \vec{u}'.$$

For 2D flows the linear stability theory uses a coordinate system (x, y) that is aligned with the local edge velocity of the undisturbed laminar mean flow such that y is wall normal. A parallel mean flow in x-direction will be considered with derivatives that only depend on the wall normal direction, e.g. $\vec{U} = (U(y), 0, 0)^T$. In boundary layer flow this is only an approximation since there is usually small flow component into the wall-normal direction, which is responsible for the boundary-layer growth. In order to find an expression for the pressure, the divergence of the Navier-Stokes equations results in

$$\nabla^2 p + 2U_y v'_x + \frac{\partial}{\partial t} (u'_x + v'_y + w'_z) + U \frac{\partial}{\partial x} (u'_x + v'_y + w'_z) - \frac{1}{Re} \left[\frac{\partial^2}{\partial x^2} (u'_x + v'_y + w'_z) + \frac{\partial^2}{\partial y^2} (u'_x + v'_y + w'_z) + \frac{\partial^2}{\partial z^2} (u'_x +$$

which reduces with combination with the continuity equation to

$$\nabla^2 p = -2U_y v'_x \quad (0.3.3)$$

The Orr-Sommerfeld equation is found by taking the laplacian of the momentum equation in the y-direction:

$$\frac{\partial}{\partial t} \nabla^2 v' + U \frac{\partial}{\partial x} \nabla^2 v' + U_{yy} v'_x + 2U_y v'_{xy} + \frac{\partial}{\partial y} \nabla^2 p' - \frac{1}{Re} \nabla^4 v' = 0$$

and using equation 0.3.3 to replace the pressure which results in

$$\left[\left(\frac{\partial}{\partial t} + U \frac{\partial}{\partial x} \right) \nabla^2 - \frac{\partial^2 U}{\partial y^2} \frac{\partial}{\partial x} - \frac{1}{Re} \nabla^4 \right] v' = 0$$

The perturbation stream function representing a single Tollmien-Schlichting wave is assumed to be of the form:

$$\psi(x, y, t) = \hat{\varphi}(y) e^{i(\alpha x - \omega t)}$$

The components of the perturbation velocity can then be expressed as:

$$u' = -\frac{\partial \psi}{\partial y} = \hat{\varphi}'(y) e^{i(\alpha x - \omega t)}$$

$$v' = \frac{\partial \psi}{\partial x} = -i\alpha \hat{\varphi}(y) e^{i(\alpha x - \omega t)}$$

Herein, α and ω are complex,

$$\alpha = \alpha_r + i\alpha_i$$

$$\omega = \omega_r + i\omega_i$$

with α_r being the wave number (wavelength $\lambda = 2\pi/\alpha_r$), ω_r the frequency and α_i, ω_i amplification rates. It can be distinguished between a spatial and a temporal theory: In the spatial theory ω is real, and amplification rates $\alpha_i < 0$ denote spatial amplified disturbances in flow direction, while in the temporal theory α is real and amplification in time are given for amplification rates $\omega_i > 0$ and given positions x . Using the spatial theory and introducing the perturbation velocities into the Navier-Stokes equations, one can obtain the Orr-Sommerfeld equation for the amplitude $\hat{\phi}$:

$$\hat{\phi}'''' - 2\alpha^2\hat{\phi}'' + \alpha^4\hat{\phi} = iRe [(\alpha U - \omega) (\hat{\phi}'' - \alpha^2\hat{\phi}) - \alpha U''\hat{\phi}].$$

Using homogenous boundary conditions for the perturbations at the wall and for large values of y , the problem of stability is now reduced to an eigenvalue problem, assuming that the mean flow, Reynolds number and frequency ω are given. Then, the solution yields the most unstable complex eigenvalue $\alpha = \alpha_r + i\alpha_i$.

A quite successful method for transition predictions was derived from observations that the location of the final transition phase is dominated by the primary instabilities with exponential growth. It has been found that the point where the boundary layer becomes fully turbulent correlates strongly with certain amplification factor of the most unstable primary wave. The findings constitute the e^N method. In the spatial theory, the overall amplification factor $A(x)/A_0$ of the perturbation amplitude A is built by an integration of the local amplification rates

$$\frac{A(x)}{A_0} = e^{-\int_{x_0}^x \alpha_i dx}.$$

This is done for a fixed number of values for the frequency ω . The N-factor is then obtained by taking the maximum value of the amplitude exponent

$$N = \max \left(-\int_{x_0}^x \alpha_i(x, \omega) dx \right).$$

The e^N methods proposed by Smith and Gamberoni [7] and Van Ingen [8] based on linear stability theory, is a popular method available for transition prediction. There are three steps in the application of the e^N method. The first step involves the computing of the laminar velocity and temperature profiles at different stream wise locations. In the second step the amplifications of the most unstable waves are calculated for each profile by the e^N method. In the third step the transition location is calculated based on the calculated amplification rates. The major problem with the e^N method is that it was developed based on the linear stability theory with an assumption that the flow is locally parallel. In addition, the value of N is not universal and needs to be determined based on experimental data (wind tunnel and also the smoothness of the test model surface). Methods based on the stability theory have one major obstacle - they need to track the growth of the disturbance amplitude along a streamline. This limitation poses a significant problem for three dimensional flow simulations where the streamline direction is not aligned with the grid. In order to get the boundary layer data a sufficient level of accuracy, an extremely high grid density is required. These methods also require well converged steady-state solution, which may not be obtainable for real-world problems involving local flow separations. Some different techniques have been employed to use these stability based methods more efficiently. One method is to generate a database of the solution of the linear stability equation for different velocity profiles in advance. The non parallel effects neglected in the linear stability theory is addressed by the linear Parabolized Stability Equations (PSE) method.

0.3.1.1 The Orr-Sommerfeld Method of Jaffe et al.

In a paper proposed by Michel (1952) [9] noted that the transition points in his data compilation seemed in all cases to correspond to a total amplification of Tollmien-Schlichting waves equal to about $A/A_0 \approx 10^4$. This fact inspired workers in computational stability to evaluate the eigenvalues for various boundary-layer profiles and to compute to growth of a given frequency. In this way Smith and Gamberoni [7] and, Van Ingen [8] verified that temporal stability theory applied to these experiments would give a total growth

$$\frac{A}{A_0} = \exp \left[\int_{x_i}^{x_{tr}} (\alpha c_i dt) \right] \approx e^9$$

This method became known as the e^9 method. Later, Jaffe et al. (1970) showed that a more realistic procedure would be to use spatial stability theory to evaluate the overall growth. Their computation with the exact velocity profiles, rather than with local-similarity approximations, gave good agreement with transition measurements when

$$\frac{A}{A_0} = \exp \left[\int_{x_i}^{x_{tr}} (-\alpha_i dx) \right] \approx e^{10}.$$

0.3.1.2 Model of Lian and Shyy [10]

This model was developed for simulation of flow around the wing of a micro air vehicle (MAV). The approach used in this model was to couple the incompressible RANS solver with the e^n method. The $k - \omega$ model of Wilcox [1] was selected for modeling the turbulence. The coupling is accomplished as follows. The computation is started with the solution of the RANS equations, while the eddy viscosity is not added to the effective viscosity. The boundary layer parameters required for the solution of the e^n method are extracted from the RANS solution to evaluate the amplification factor. Once the threshold value of the n-factor is reached, the flow is allowed to become turbulent by multiplying the eddy viscosity with the intermittency factor and adding it to the effective viscosity. The intermittency in this case is based on the assumption that the initial disturbance is small and that the boundary layer is thin.

0.3.1.3 Model of Artur and Atkin [11]

This method is based on linear stability theory applied within a RANS framework. The viscous flow over the body is first calculated with an initial guess of the transition onset location. A series of pressure distributions is extracted from the RANS solution at different positions. These pressure distributions are fed into a boundary layer code to predict the boundary layer parameters with great accuracy and fidelity. The stability analysis, together with the “n” factor criterion is conducted to yield the transition location. This information is then passed onto the RANS solver for further solution. This process is repeated until the transition location and the pressure distribution are converged. This method does not have any intermittency model to predict the nature of the region of transition.

0.3.2 Transition models with specified transition onset

The transition region models in this section are unable to predict the location of the transition. The transition location is determined from an empirical data or linear stability equation computation. The transition region is modeled by modifying existing turbulence models. In Ref [12] six transition models were implemented into a commercial Navier-Stokes code. These models were used to simulate hypersonic experimental cases that included transition on a cone at Mach 6, a compression ramp at Mach 10, and five flared cone test cases at Mach 7.93. The six models are as follows:

1. **Baldwin-Lomax algebraic turbulence model [12]** - This model predict the transition region by turning off the turbulence model for the laminar region by setting the eddy viscosity equal to zero and then just turning it on at the transition point. In most of the cases this model adequately predicted the peak heat transfer, but under predicted the transition length.
2. **Warren, Harris and Hassan one equation model [13]** - This model attempts to include the effect of second mode disturbances in addition to the first mode. The model was used to simulate cases in which the first mode disturbances dominate the transition process ($M < 4$) and cases in which the second modes are dominant ($M > 4$).

3. **Wilcox $k-\omega$ turbulence model** [1] - The prediction of the transition region is obtained by triggering the boundary layer at a given point by decreasing the value of the dissipation so as to destabilize the boundary layer and cause transition. The application of this model in Ref [12] showed that it was difficult to trig the boundary layer at the desired location due to sensitivity to the initial conditions.
4. **Schmidt and Patanker production term modifications** [14] - Schmidt and Patanker have developed modifications to the production term in the turbulent kinetic energy equation of the Lam and Bremhorst $k-\epsilon$ model [15]. These modifications limited the production of the kinetic energy. For the use of this model a trial and error method was needed to make transition occur at the desired position by varying the inlet conditions.
5. **Algebraic transition model** [16] - This model predicts transition by multiplying the eddy viscosity by a transition function before adding it to the fluid viscosity. This function is related to the momentum thickness growth. In test cases with severe adverse pressure gradients, where the momentum thickness decreases, the model did not produce transition. It was found that this model did not perform well with two equation models.
6. **Linear combination transition model** [17] - This model is based on the concept that the transition flow is a combination of the laminar and turbulent flow fields. The contribution from laminar and turbulent values is based on the intermittency factor. This model requires a complete laminar flow simulation be run first, followed by a turbulent one, with the turbulent boundary layer starting at the point of transition. The transitional solution, for example, the mean velocity U , is generated as follows:

$$U = (1 - \Gamma)U_L + \Gamma U_T$$

The subscripts L and T stand for values in the laminar and turbulent boundary layers, respectively. The maximum heat transfer was not predicted in the test cases simulated in [12].

0.3.3 Transition models with onset prediction capability

There is no fundamental theory of transition, but experiments and correlations which try to predict a fully turbulent flow, such as $Re_{x,tr}$ or $Re_{\theta,tr}$ as a function of the following parameters:

1. Pressure gradient
2. Free stream turbulence
3. Wall roughness
4. Mach number
5. Wall suction or blowing
6. Wall heating or cooling

Effect of pressure gradient

Consider the problem sketched in figure 0.1.1. We assume $U(x)$ is known, the walls are smooth, impermeable and unheated. The boundary layer will be initially laminar and will become unstable at point x_i . At this point Tollmien-Schlichting waves will first appear, and will grow until the point of transition x_{tr} , is reached. We wish to predict x_{tr} , using x_i as an input if necessary. In the following lines several methods are described.

0.3.3.1 The Two-step method of Granville

The computation of x_i is done by following $H(x)$ from Thwaites' method until it hits the Re_{crit} correlation of Fig. (). Then while monitoring $Re_{\theta}(x)$, Granville suggests computing a mean Thwaites' parameter,

$$\lambda_m = \frac{1}{x_{tr} - x_i} \int_{x_i}^{x_{tr}} \lambda(x) dx$$

where $\lambda = \theta^2 (dU/dx)/\nu$. The x_{tr} occurs when Re_θ strikes Granville's transition data,

$$Re_\theta(x_{tr}) \approx Re_\theta(x_i) + 450 + 400e^{60\lambda_m}.$$

For adverse gradient $\lambda \approx -0.1$ the last term is negligible and the transition point is close to x_i . For favorable gradients the last term is large and the transition occurs far downstream.

0.3.3.2 The One-Step Method of Michel

This method is chosen due to its low computational cost. Despite the low cost, the correlations maintain an acceptable level of accuracy. The Michel criterion [9] is based on experimental correlation of the local Reynolds number and momentum thickness Reynolds number with the transition point. Transition onset takes place where

$$Re_{\theta,tr} = 1.174 \left(1 + \frac{22400}{Re_{x,tr}} \right) Re_{x,tr}^{0.46}$$

The local Reynolds number using the distance from the stagnation point as the reference length is

$$Re_{x,tr} = \frac{\rho u x}{\mu}$$

here x is the distance along the body (an airfoil for example) surface from the stagnation point to the testing point for transition. The momentum thickness of the boundary layer is

$$\theta = \int_0^\infty \frac{\rho u}{(\rho u)_{edge}} \left[1 - \frac{\rho u}{(\rho u)_{edge}} \right] dy$$

The Reynolds number using the momentum thickness as the reference length is

$$Re_{\theta,tr} = \frac{\rho u \theta}{\mu}$$

At each computation node the Reynolds numbers are calculated and Michel's criterion is assessed. Once satisfied turbulence is tripped and further downstream nodes are considered turbulent.

0.3.3.3 The One-Step Method of Wazzan et al.

The success of correlating Re_{crit} for different cases led Wazzan et al (1979, 1981) to propose a similar correlation for the transition Reynolds number. One computes $H(x)$ by any laminar boundary-layer method i.e., Thwaites. Transition is predicted when Re_x hits the following curve fit:

$$\log_{10}(Re_{x,tr}) \approx -40.4557 + 64.8066H - 26.7538H^2 + 3.3819H^3$$

for $2.1 < H < 2.8$.

Effect of Free stream Turbulence

The parameter characterizing free stream turbulence level is defined as $T = q/U$ where $q = \left[\frac{1}{3} (\overline{u'^2} + \overline{v'^2} + \overline{w'^2}) \right]^{1/2}$ in which U is the mean free stream velocity and u' , v' , w' are the fluctuating velocities in the free stream. The effect of T on transition is very strong. Free stream disturbances are due to grid generated turbulence, acoustic noise, excited standing waves and excited traveling waves.

0.3.3.4 The correlation of Van Driest and Blumer

Van Driest and Blumer [18] theorized that transition occurs when the Reynolds number associated with maximum vorticity in the boundary layer,

$$Re_\omega = \left(\frac{\omega y^2}{\nu} \right)_{max}$$

reaches a critical value to be correlated with free stream turbulence. By relating Re_ω to the shape of the profile, Van Driest and Blumer derived the following formula for flat plate transition:

$$Re_{x,tr}^{1/2} = \frac{-1 + \sqrt{1 + 132500T^2}}{39.2T^2}$$

where T is to be taken as a fraction.

0.3.3.5 The correlation of Dunham

Dunham [] collected data on combined free stream turbulence and pressure gradient effects, while studying boundary layer transition on turbo machinery blades. The correlation is as follows:

$$Re_{\theta,tr} \approx (0.27 + 0.73e^{-80T}) \left[550 + \frac{680}{(1 + 100T - 21\lambda_{tr})} \right]$$

for $\lambda < 0.04$, where λ is the Thwaites parameter.

The following models not only simulate the characteristic of the transition region, but also predict the onset of transition.

0.3.3.6 David C. Wilcox - Simulation of Transition with a Two-Equation Turbulence Model [1]

The standard approach is to view development of a transition model and a low-Reynolds number turbulence model as two separate issues. The strongest argument in favor of this approach is simply that all spectral effects are lost in the time-averaging process used by turbulence models. Tollmien Schlichting waves cannot be distinguished by a turbulence model. Since a given boundary layer is unstable to perturbations that fall in a specific range of frequencies, conventional turbulence models, which distinguish only magnitude and an average frequency, can never be certain if a given perturbation will actually cause transition. However, if we implement two separate models, one for the transition region and another for the developing turbulent region, achieving a smooth joining of the two model's predictions presents an additional complication. This complication can be avoided if we view both issues as low-Reynolds-number phenomena that can be addressed in the context of a single model. The strongest argument for this approach is that we can use the same model to describe a smooth transition from laminar to fully turbulent flow, including the transitional region.

This is very clear that this approach does not have sufficient physical foundation to describe the onset of transition. The conceptual reason for this reservation is as follows. Using the single length scale implied by a typical two-equation turbulence model is much less satisfactory for transitional flows than for turbulent flows. That is, production and dissipation processes come from different parts of the turbulence spectrum. Large eddies are primarily responsible for production, whereas the smallest eddies dissipate turbulence energy into internal energy. In a turbulent flow, the largest eddies also control the rate of dissipation by way of the cascading of energy down the spectrum to the smallest eddies. That, there is a degree of universality to the turbulence spectrum for turbulent flows, provided the Reynolds number is large enough to permit a distinct inertial sub range. By contrast, it is very unlikely that such a universal spectrum exists in a transitional flow, and certainly not in the earliest stages of transition.

Two equation turbulence models appear to give useful results for a much wider range of turbulent flows. This work describes the nonlinear growth of disturbances once transition has begun.

0.3.3.7 Suzen and Huang model [19]

This model uses a transport equation for the intermittency factor. This equation gives a realistic variation of the intermittency in the cross-stream direction. The intermittency transport equation includes source terms from two different models: the steelant and Dick model [20] and the Cho and Chung model [21]. This model is incorporated into the Navier-Stokes solver by multiplying the eddy viscosity obtained from the turbulence calculations with the intermittency factor. The Menter's (SST) model was used to calculate the turbulent quantities. The onset of transition was determined by comparing the local Reynolds number with a transition onset Reynolds number calculated using the correlation of Huang and Xiong [22]. This model is not a single point model since it uses the free stream turbulence intensity value to calculate the transition onset Reynolds number, which requires global parameters.

0.3.3.8 Transport Equation for Laminar Kinetic Energy

A very interesting transition modeling approach that has recently been proposed is based on modeling the development of the pre-transitional laminar fluctuations all the way up to the onset of transition and then into the turbulent region. The idea was originated by Mayle and Schulz [23] who proposed a transport equation for the kinetic energy of the laminar fluctuations upstream of transition. The onset of transition was judged to occur once the laminar fluctuations in the boundary layer reached a certain level. Again the main problem with the Mayle and Schulz [23] model was that the source term in the transport equation was based on non-local values such as the free stream velocity. Walters and Leylek [24] used Mayle and Schulz's (1997) ideas to develop a locally formulated transport equation for the laminar kinetic energy which represents the magnitude of non-turbulent stream wise fluctuations in the pre-transitional boundary layer. This laminar kinetic energy equation was then coupled to a turbulent kinetic energy (k) and a turbulent eddy frequency (ω) equation. The model automatically predicts the onset of transition without any intervention from the user and is based strictly on local variables. It has not been extensively validated except for a few flat plate test cases and a turbine blade. However, the initial results of this model were promising and indicate that the model appears to have the correct sensitivity to free stream turbulence.

Walters and Leylek model [24]

This model is based on the concept that bypass transition is caused by very high amplitude stream wise fluctuations. Mayle and Schulz proposed a second kinetic energy equation, k_L , to describe these fluctuations. In the near-wall region, the turbulent kinetic energy, k_t , was split into small scale energy and large scale energy. For the onset of transition, a parameter is calculated from k_t , the kinematic viscosity and the wall distance. When this parameter exceeds a certain threshold, transition is assumed to start. The onset of transition is associated with the reduction of the laminar kinetic energy and the consequent increase of k_t . This model was incorporated into a RANS flow solver. It yields good results for cases with high pressure gradients. Advantages of this method that it is based on a RANS framework and is a single point transition model meaning that it requires only local information. Since this transition model is developed based on the low-Re $k - \epsilon$ model, the embedded viscous sublayer formulation coupled with the added transition prediction capability cannot be calibrated independently.

0.3.3.9 R.B Langtry and F. R. Menter - Transition Modeling for General CFD Applications [3]

This transition model is correlation based and is built strictly on local variables. As a result the transition model is compatible with modern computational fluid dynamics techniques such as unstructured grids and massively parallel execution. The model is based on two transport equations, one for the intermittency and one for a transition onset criterion in terms of momentum-thickness Reynolds number. The central idea behind the new approach is that Van Driest and Blumer [18] vorticity Reynolds number concept can be used to provide link between the transition onset Reynolds number from an empirical correlation and the local boundary-layer quantities. As a result, the model avoids the need to integrate the boundary layer velocity profile to determine the onset of transition. The vorticity or alternatively the strain rate Reynolds number which is used in the present model is defined as follows:

$$Re_v = \frac{\rho y^2}{\mu} \left| \frac{\partial u}{\partial y} \right| = \rho y^2 S$$

where y is the distance from the nearest wall. Because the vorticity Reynolds number depends only on density, viscosity, wall distance and the shear strain rate, it is a local property and can be easily computed at each grid point. A scaled vorticity Reynolds number Re_v in a Blasius boundary layer is $y/\delta \approx Re_v/2.193Re_\theta$. The scaling is chosen to have a maximum of one inside the boundary layer and this is achieved by dividing the Blasius velocity profile by the momentum-thickness Reynolds number and a constant of 2.913. In other words, the maximum of the profile is proportional to the momentum-thickness Reynolds number and can therefore be related to the transition correlations [25] as follows:

$$Re_\theta = \frac{\max(Re_v)}{2.193Re_\theta}$$

The function Re_v can be used on physical reasoning, by arguing that the combination of y^2S is responsible for the growth of disturbances inside the boundary layer, where is μ/ρ is responsible for their damping. As y^2S grows with the thickness of the boundary layer and μ stays constant, transition will take place once a critical value of Re_v is reached. The connection between the growth of the the disturbances and the function Re_v was shown by Van Driest and Blumer [18] in comparison with experimental data. The concept of linking the transition model with experimental data has proven to be an essential strength of the model and this is difficult to achieve with closures based on a physical modeling of these diverse phenomena.

This transition model is built on a transport equation for intermittency, which can be used to trigger transition locally. The first transport equation includes two terms that control production. These are F_{length} , a parameter which controls the length of transition zone, and Re_{θ_c} which is the momentum thickness Reynolds number at the point where the intermittency starts to increase in the boundary layer. These two variables are calculated from empirical functions of the transition momentum thickness Reynolds number Re_{θ_t} . In addition, a second transport equation is solved for the transition onset momentum-thickness Reynolds number. this is required to capture the non local influence of the turbulence intensity, which changes due to the decay of the turbulence kinetic energy in the free stream, as well as due to changes in the free stream velocity outside the boundary layer. This second equation is essential as it ties the empirical correlation to the onset criteria in the intermittency equation.

0.3.3.10 The model of Lodefier et al. [26]

This model is based on the concept of pre-transitional fluctuations similar to the Walters and Leylek model. However, this model uses the concept of intermittency to describe the transition region, as was proposed by Steelant and Dick [27]. The production term of this intermittency equation was modified by multiplying it with a factor in order to locate the transition onset. This factor is zero before the start of transition and rapidly goes to unity after the onset point. Similar to Langtry and Menter model [3], the vorticity Reynolds number is used in triggering transition. Unlike [3], the equation used to calculate the critical value of Re_{θ_t} for transition is calculated from the local free stream turbulence intensity and not from a transport equation. The empirical correlation used for Re_{θ_t} does not include a pressure gradient term. The model is incorporated into the KW-SST model both by multiplying the eddy viscosity with the intermittency and by modifying the production terms of the k and w equations. These modifications are used to ensure that the turbulence quantities have small non-zero values at the start of transition. The main disadvantage of this model is that it uses the free stream intensity to determine the onset of transition, which makes the model non-local unlike [3].

0.3.3.11 The $\gamma - Re_\theta - SA$ model of Medida et al. - [28]

The original $\gamma - \overline{Re_{\theta_t}}$ transition model was developed by Langtry et al. [3] for use with the $SST - k - \omega$ turbulence model. One advantage of this model over many other transition models is that it does not require the integration of a boundary layer followed by a search for critical Re_θ at which transition onset begins. Furthermore, because this model allows intermittency to vary across the boundary layer, it is able to capture transition triggered by a laminar separation bubble

without need for further correction. This is particularly advantageous in low speed flows, where separation bubbles are frequently the cause of transition. The model is correlation based and provides a convenient framework wherein users may insert proprietary or internal correlations.

The $\gamma - \overline{Re_{\theta t}} - SA$ model, introduced by Medida et al. [28] adapts this method to work with the one equation Spalart-Allmaras turbulence model. In addition to the RANS equations and turbulence model equation, the $\gamma - \overline{Re_{\theta t}} - SA$ model requires the solution of two transport equations. The first is for intermittency, γ , a quantity which varies from zero to one and represents the probability of turbulent flow at a given location. The second is for the transition momentum thickness Reynolds number $\overline{Re_{\theta t}}$, the purpose of which is to convect the effects of turbulence intensity from the free stream into the boundary layer.

The $\gamma - \overline{Re_{\theta t}} - SA$ model has been implemented by Anikate C. Aranake et al. [29], and their work includes few validations that confirm the model's credibility in transitional flows such as those seen in the wind turbine applications.

0.3.3.12 Jan Windte, Rolf Radepiel and Ulrich Scholz - RANS Simulation of The Transitional Flow Around Airfoils at Low Reynolds Numbers for Steady and Unsteady Onset Conditions

In this paper RANS computations around airfoils are presented for flows where transition takes place across a laminar separation bubble. Transition locations are found employing the e^N method and a linear stability solver that uses the velocity and temperature profiles from the RANS solution.

Based on the literature survey, it is concluded that LCTM and the Walters and Leylek model constitute the formulations best suited for production CFD codes because they are both single-point models that can be easily incorporated into the existing RANS CFD codes. Both of these models provide an estimate of the location for turbulence transition and enable the CFD codes to simulate the flow characteristics in the transition region. These two models have been found to produce transition locations that respond properly to changes in free stream turbulence intensity and local pressure gradients.

Part I

Validation of Menter-SST and KKL Transition models

0.4 Flat plate test cases

This part of the work is devoted to the validation of the two turbulence models for various 2D test cases. The Menter-SST and KKL transition models has been used to predict the transition with T3 series of experimental flat plate test cases. The radius of the rounded leading edge was 0.75 mm and the flat plate had a length of 1.5 m. These experiments were performed at Rolls-Royce in the 1990's [30]. All the T3 series of tests had a free stream turbulence intensities of 1% or greater, and as a result bypass transition was the dominant transition mode. In order to test the transition models ability to predict natural transition the Schubauer and Klebanoff (1955) flat plate experiment has also been computed. The T3 measurements were performed on a flat plate subjected to different levels of free stream turbulence and pressure gradient. Test cases T3A, T3B, and T3Am had a zero stream wise pressure gradient with free stream turbulence intensities of 3%, 6% and 1%, respectively. The different free stream turbulence levels were imposed by turbulent grids which inserted into the wind tunnel test section upstream of the flat plate. The Schbauer and Klebanoff zero pressure gradient flat plate experiment was performed with a relatively quiet wind tunnel with a 0.1 turbulence intensity near the transition location. The T3C test cases had a stream wise pressure gradient that is achieved by contouring the upper wall (of the tunnel) and thus alter the development of the flat plate boundary layer. A summery of the inlet conditions used for each test case is summarized in table 1.

A grid independence study was performed for a single test case. In addition, a number of sensitivity studies were performed with the transition model on the effect of y^+ , wall normal expansion ratio and stream wise grid refinement. It was found that in order for grid independent results to be achieved the maximum y^+ should not exceed 1, the wall normal stretching factor should be between 1.1 and 1.15 and at least 1000 cells along the plate in order to properly capture the laminar, transitional and turbulent boundary layer development. The mesh used for the cases T3A, T3B and T3Am (zero pressure gradient) is presented in figure 0.4.1 and the mesh used for the T3C4 test case is presented in figure 0.4.2.

Case	Inlet Velocity (m/s)	Turbulence Intensity (%)	μ_t/μ	Density (kg/m ³)	Dynamic Viscosity (m ² /s)
T3A	5.4	3.3	12.0	1.2	1.8×10^{-5}
T3Am	9.4	6.5	100.0	1.2	1.8×10^{-5}
T3B	19.8	0.874	8.72	1.2	1.8×10^{-5}
Schubauer and Klebanof	50.1	0.3	1.0	1.2	1.8×10^{-5}
T3C2	5.29	3.0	11.0	1.2	1.8×10^{-5}
T3C3	4.0	3.0	6.0	1.2	1.8×10^{-5}
T3C4	1.37	3.0	8.0	1.2	1.8×10^{-5}

Table 1: Inlet condition for the flat plate test cases

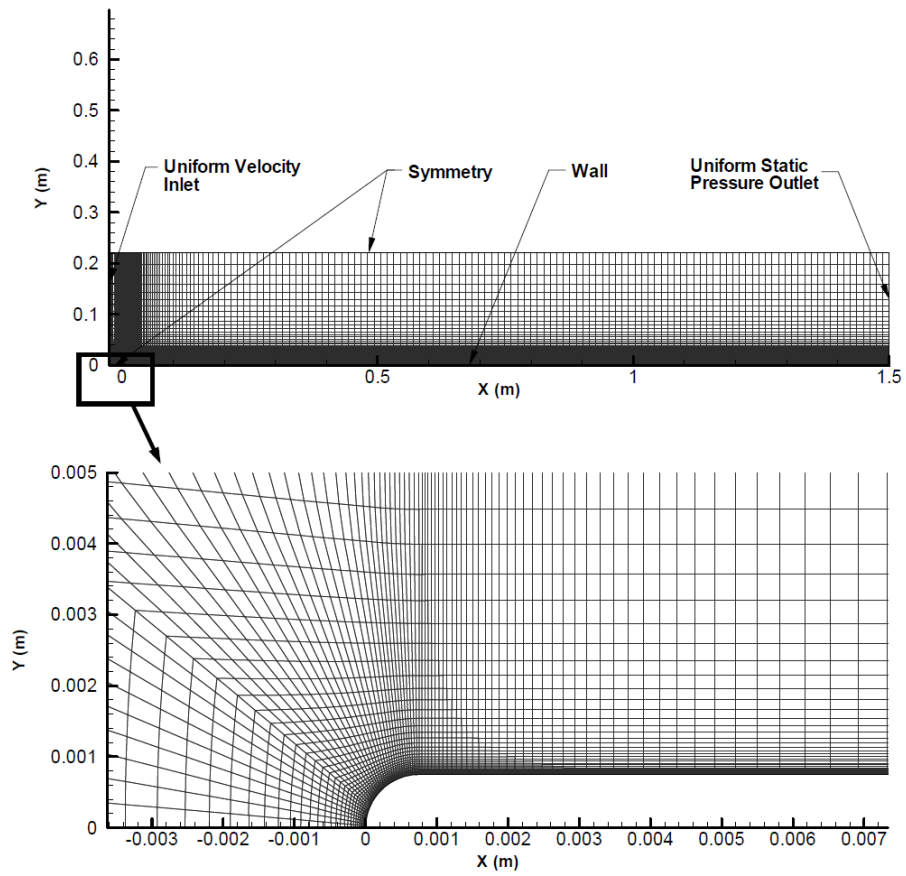


Figure 0.4.1: Flat plate mesh used for the T3A, T3B and T3Am test cases

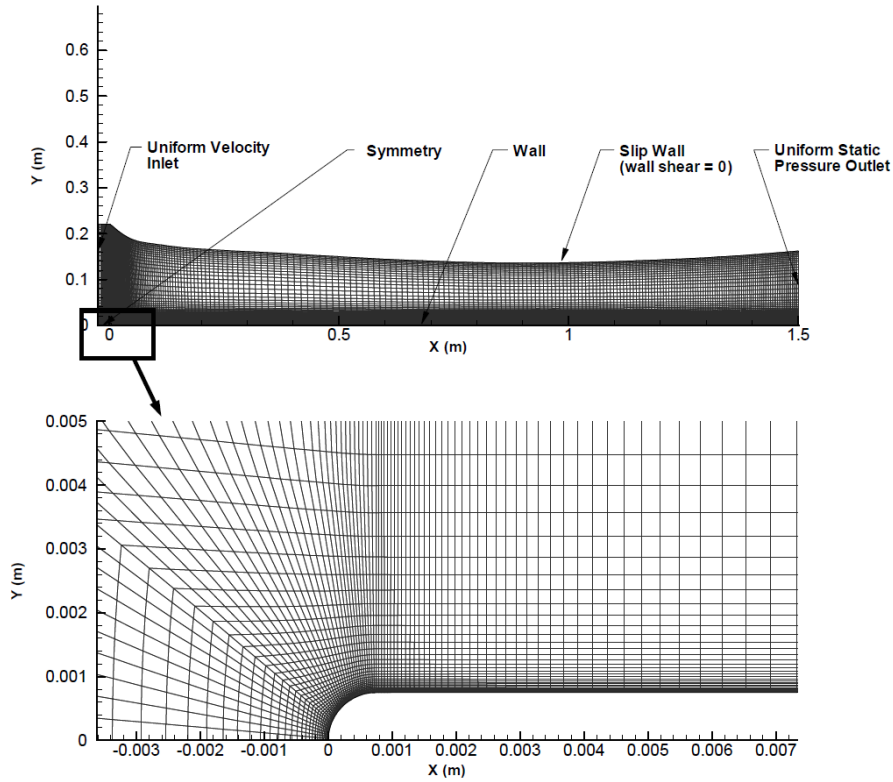


Figure 0.4.2: Flat plate mesh used for the T3C4 test case along with a magnified view of the leading edge region.

The effects of the grid refinement on the quality of the numerical solution are described in figure 0.4.3 for the three models. The transition location checked for three grid levels, while using the KKL transition model for the T3Am test case. It is clearly seen that the numerical solution of the transition onset is highly sensitive to the number of cells in the stream wise direction. The difference in the heat transfer values obtained in the three grid levels for both models is significant while moving from $h_{min} = 100\mu m$ to $h_{min} = 10\mu m$, while h_{min} is the first cell's height close to the body. The difference between $h_{min} = 10\mu m$ and $h_{min} = 1\mu m$ is minor and grid resolution studies confirmed that the computed skin friction values are grid converged. The total number of cells for the final grids is about 300,000.

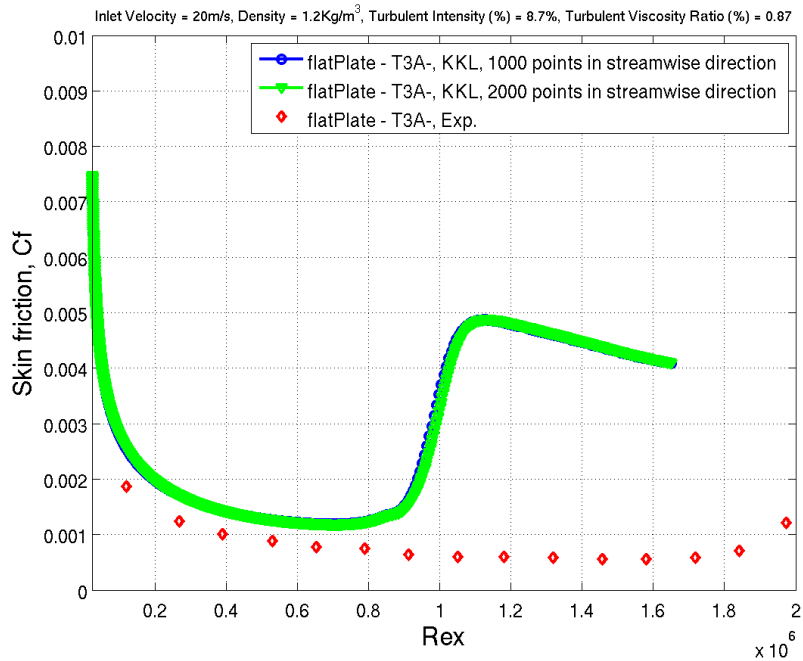


Figure 0.4.3: Grid dependence study on skin friction distributions on T3Am test case at $Tu=6.5\%$.

0.4.1 Zero pressure gradient test cases

A flow simulation was conducted by using the Fluent commercial software, which includes both KKL and Menter-SST transition models. The skin friction was computed for cases T3A, T3Am, T3B and Schubauer and Klebanoff with zero pressure gradient in the axial direction. These test cases had leading edge free stream turbulence intensities of 6.5%, 3.3%, 0.87% and 0.3% respectively. As a result the transition location moves downstream for lower free stream turbulent intensities. In general, the agreement with the experimentally measured skin friction and transition location is not good for the first ($Tu=3.3\%$) and third ($Tu=0.87\%$) cases. The KKL transition model predicted the transition onset much better than the Menter-SST model. For the low turbulence intensity (T3A) the transition location was predicted earlier than the experiment results, for both models. However, the KKL model results are much closer to the experiment values. For the high turbulence intensity case (T3B, figure 0.4.6) the laminar skin friction tends to be over predicted. This is probably due to the large values of free stream eddy viscosity values.

Results of the Schbauer and Klebanoff test case are shown in Figure 0.4.7. This test case performed in a relatively quiet wind tunnel and had a free stream turbulence intensity of only 0.1% near the transition location. However both models do not predict the transition onset at all. Even if the number of cells in the stream wise direction is doubled and the $y+$ values were lowered to nearly 0.1, no transition predicted what so ever.

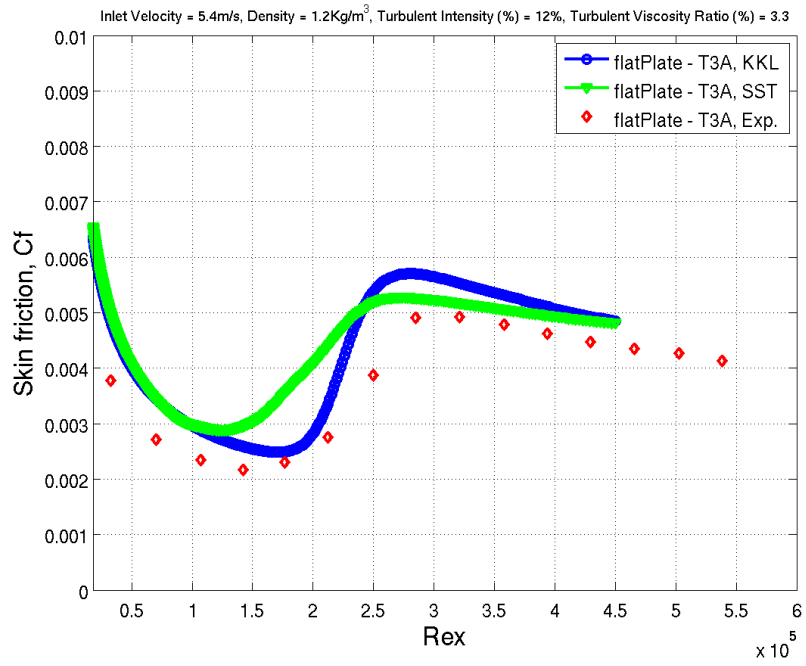


Figure 0.4.4: T3A test case (Tu=3.3%)

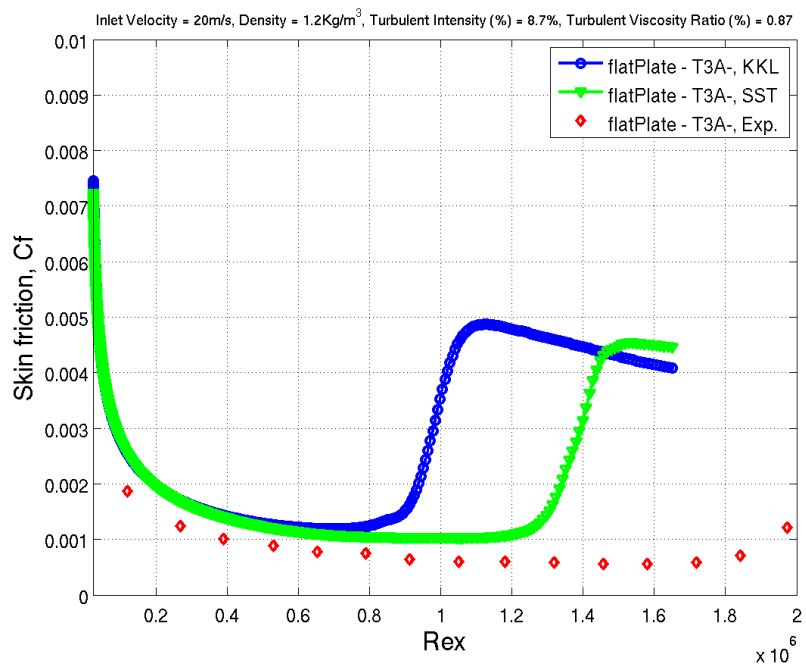


Figure 0.4.5: T3Am test case (Tu=6.5%)

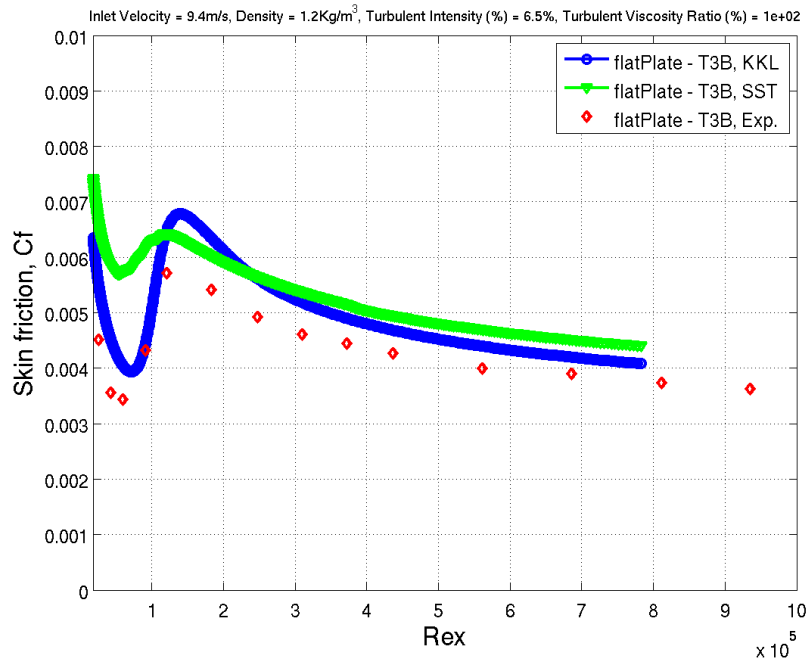


Figure 0.4.6: T3B test case (Tu=0.874%)

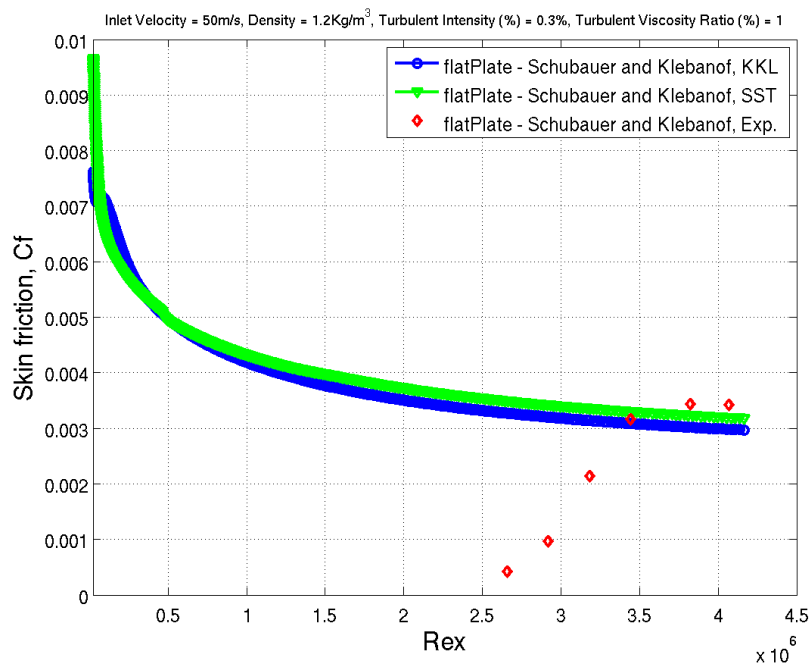


Figure 0.4.7: Schubauer and Klebanoff test case (Tu = 0.3%)

0.4.2 Pressure gradient test cases

The computed skin friction coefficient for the T3D2 test case is compared to the experimental results in figure 0.4.8. The transition location is downstream because of the relatively low Reynolds number. Both transition models does not predict well the favorable pressure region,

while the skin friction values obtained are more than twice than the experiment values. The experimental transition onset is located nearly 0.9 m from the leading edge while the KW-SST model predicted the transition onset slightly upstream. In the adverse pressure gradient the predicted transition is shorter.

The results of the T3C3 case is compared to the experimental results in figure 0.4.9. The Reynolds number was lower than the T3C2 case and the transition occurs upstream. Also in this case the transition onset was not predicted well by both models. For the T3C4 test case (see Figure 0.4.10), the Reynolds number is lower than the previous two test cases and the laminar boundary layer separates at a Re_x of 130000. The computed transition onset is not in good agreement with the experimental results. Both models predict the transition at Re_x of 90000, earlier than the experimental values. In addition, the transition length is shorter than obtained in the experiment. This test case concludes the flat plate validation of the KKL and KW-SST models. Both models has been shown a moderate performance in predicting the combined effects of free stream turbulence and strong pressure gradients on the transition. In some cases the results obtained by the KW-SST model are closer to the experimental values than those obtained with the KKL model.

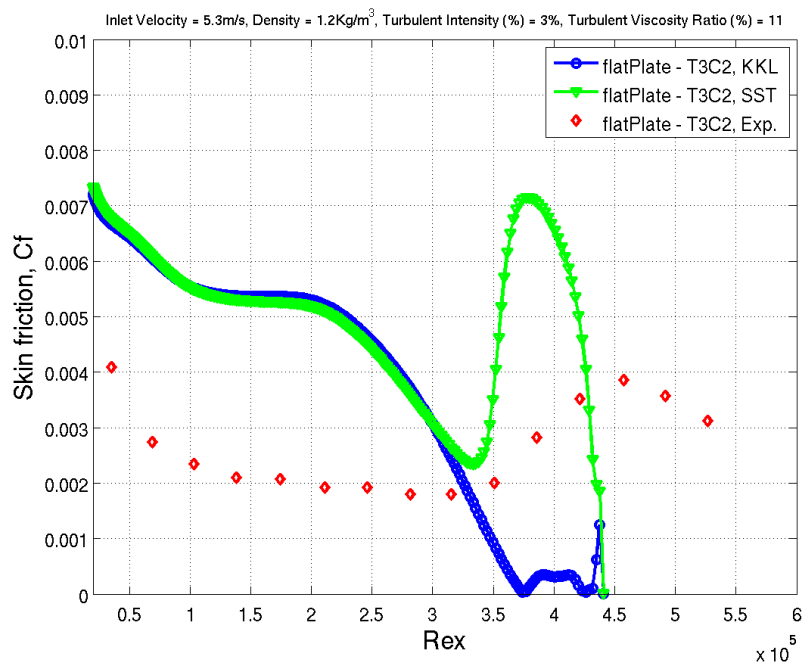


Figure 0.4.8: T3C2 test case ($Tu=3.0\%$)

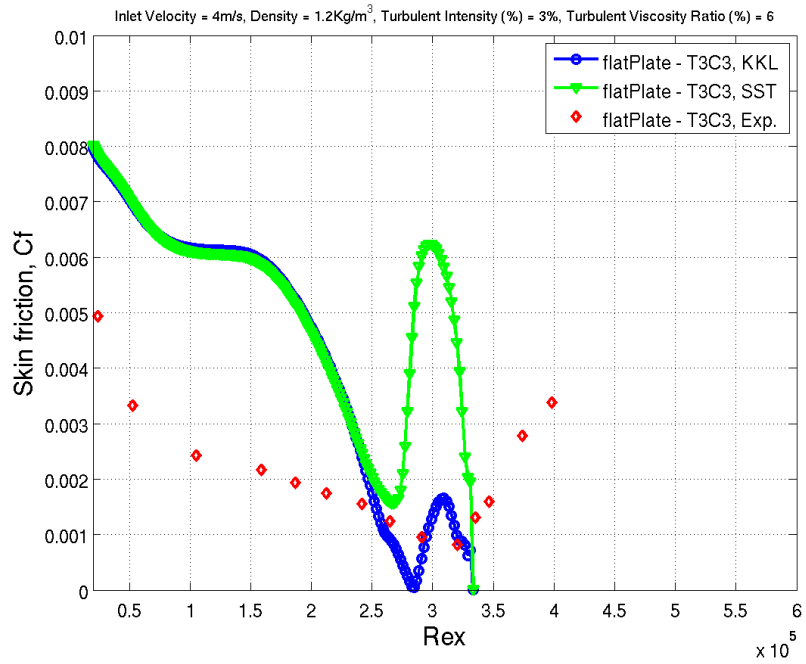


Figure 0.4.9: T3C3 test case (Tu=3.0%)

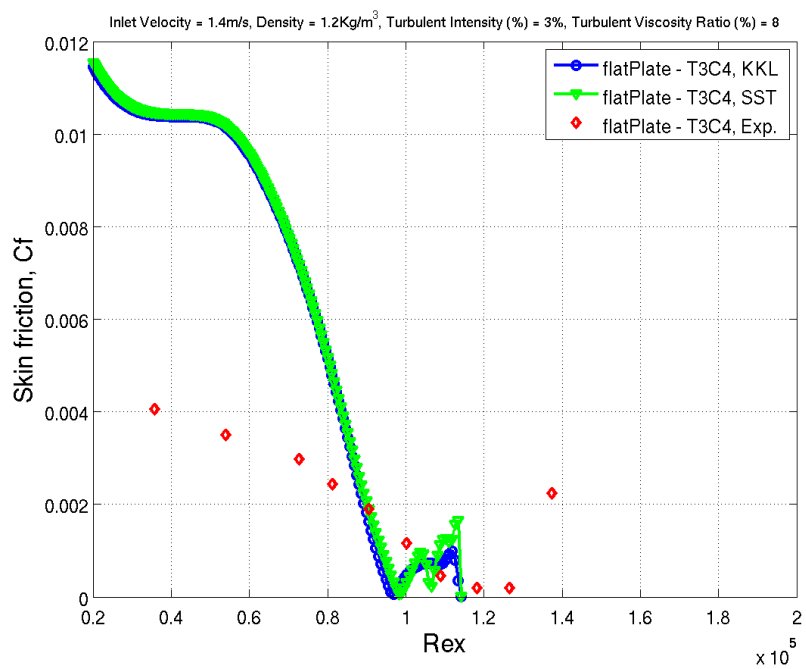


Figure 0.4.10: T3C4 test case (Tu=3.0%)

0.5 AerospitaliaA - 2D Airfoil test case

The AerospitaliaA airfoil was designed at Aerospitalia in 1986 and was tested in the Onera F1 wind tunnel [31]. The grid used for the present computation is shown in Figure 0.5.1 and consists

of approximately 100000 cells. The grid in the computation had a maximum y^+ of approximately unity, wall normal expansion ratios between 1.02 and 1.1 and at least 100 cells in the stream wise direction in order to properly resolve the laminar, transitional and turbulent boundary layers. The inlet conditions are summarized in Table 2. In this experiment test case no boundary layer trips were placed on the suction side of the airfoil. Consequently a laminar boundary layer develops and terminates at about 12% of chord. The skin friction values obtained with KKL and SST transition are compared with the experimental values in Figure 0.5.2. Both transition models predicts the transition onset at 8% chord length and not 12% as in the experiment. The lift and drag coefficients obtained with the the KW-SST model are $L = 1.52$ and $D = 0.0251$, and the results with the KKL model are: $L = 1.647$ and $D = 0.0240$. These compare quiet well with the experimentally measured values of $L = 1.562$ and $D = 0.0208$.

Rex ($\times 10^6$)	Mach	AoA (deg)	Chord (m)	Turbulence Intensity (%)	μ_t/μ
5.4	0.15	13.1	0.6	0.2	10.0

Table 2: Inlet condition for the Aerospatiale A test case.

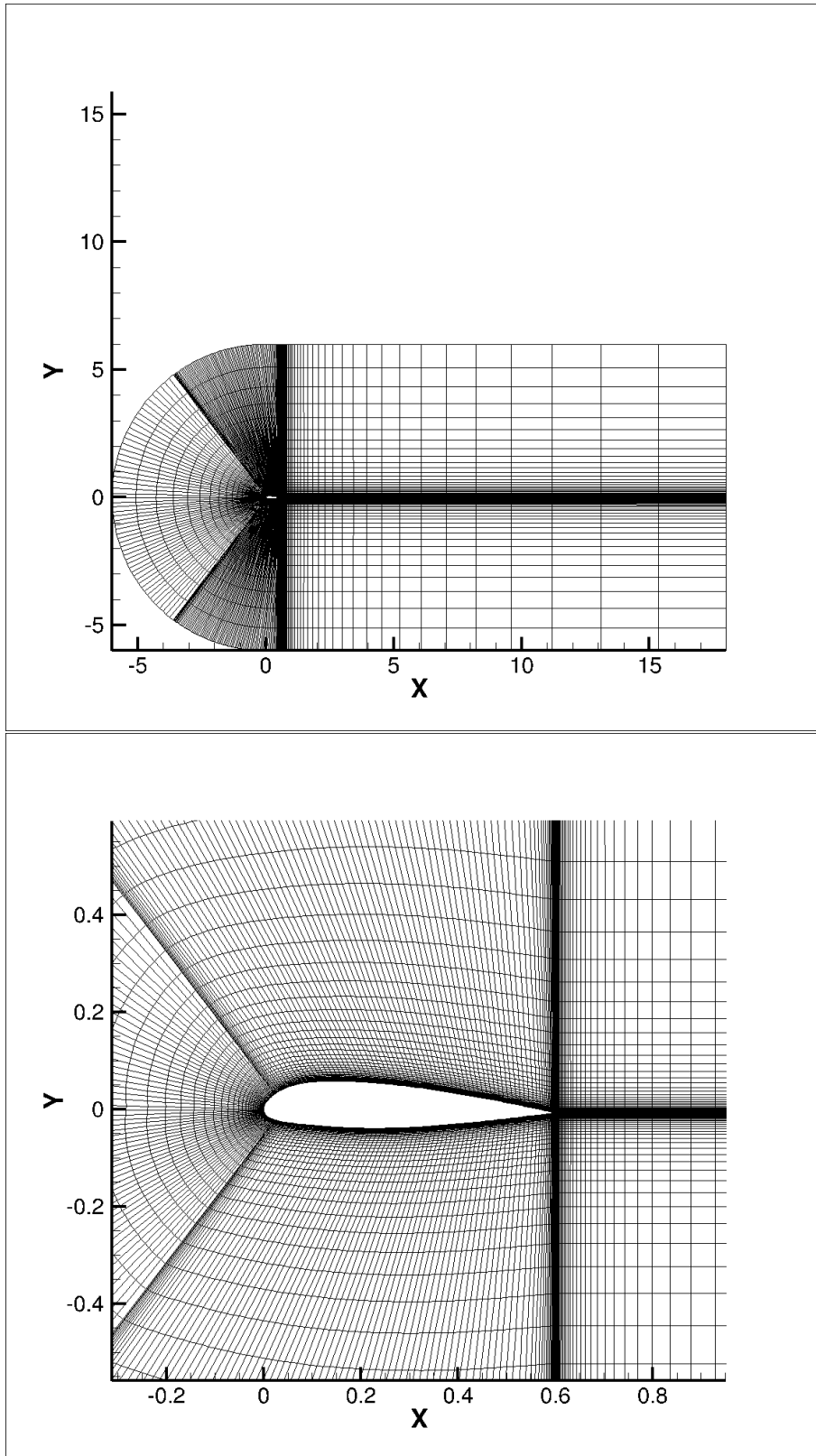


Figure 0.5.1: Aerospatiale A mesh test case along with a magnified view of the leading edge region.

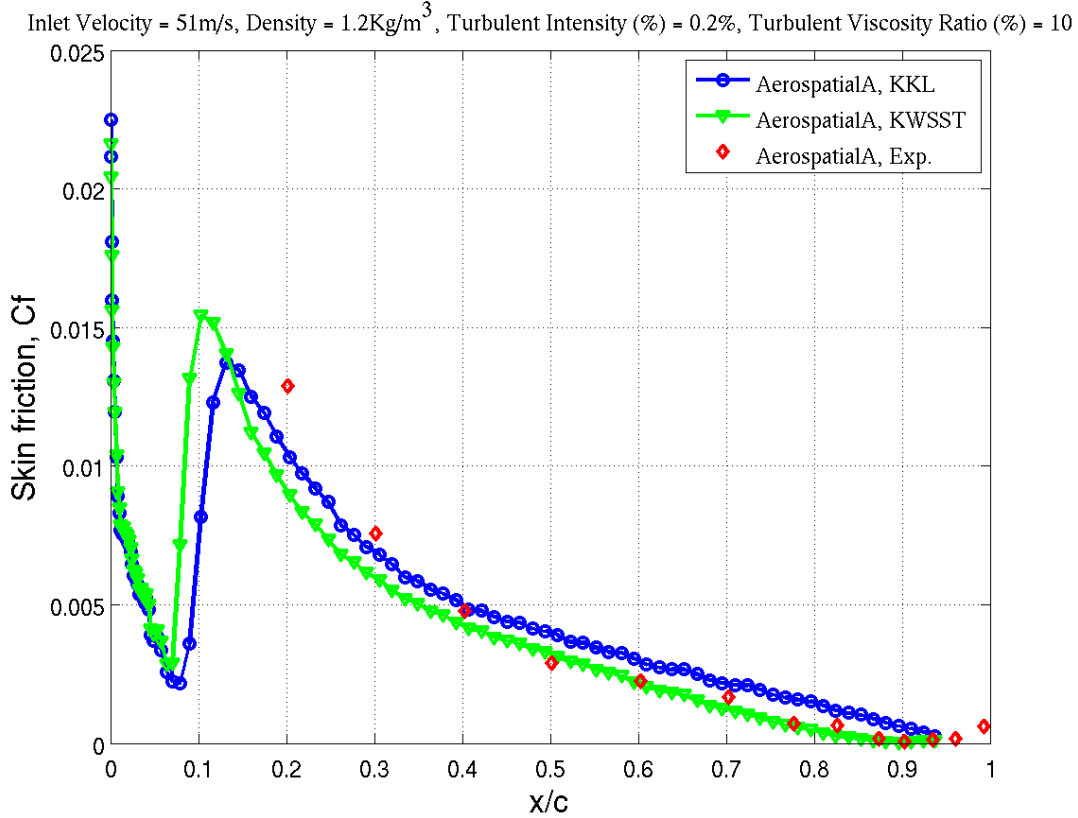


Figure 0.5.2: Skin friction on the suction side of the Aerospatiale A airfoil.

0.6 Summery

This document reviewed several transition modeling approaches. The review highlighted the difficulty in combining classical CFD to transition models. This difficulty arises from the locality of CFD algorithms that conflicts with the modeling of transition as a process that exists along streamlines. The main requirements for a fully CFD compatible transition model have been identified. The more widely used transition models have been outlined, highlighting their benefits and shortcomings. Both the Walters-Leylek model and LCTM were selected for evaluation in this study. The transition model of Menter satisfied most of the requirements of a fully CFD compatible transition model. The main limitation of the Menter transition model is the accuracy of the empirical correlations, in which the physics transition is entirely contained. The transpose equations do not attempt to model the physics of the transition process unlike turbulence models, but form a framework for an implementation of correlation-based models into general CFD methods. The other promising approach in predicting transition is the Walters-Leylek model, the laminar kinetic energy approach. This method is based on local variables, but so far it has not been extensively validated. However, the preliminary results indicate that the model appears to have a correct sensitivity to the free stream turbulence levels. It is expected that the concept of a laminar kinetic energy will be an active area of transition research in the future.

The Walters-Leylek and LCTM models were tested in Fluent commercial software for two sets of benchmark test cases. For flow over a flat plate, the Walters-Leylek and LCTM were shown to properly account for transition to different turbulence intensity values. The result show that both models can capture the onset as well as the turbulence transition very well when the turbulence level is moderate ($\sim 3\%$). As the upstream turbulence intensity is high ($\sim 7\%$) or low ($\sim 0.3\%$) prediction of the onset location is not good and the transition region starts to deviate from the test data. To date, none of the transition models have been shown satisfied results in

terms of onset location and transition region length, for the flat plate as well as Aerospacial A airfoil. However, the range of applicability and validity for both transition models is questionable. Further, investigations are needed to develop a more complete assessment of these two transition models.

Bibliography

- [1] D. C. Wilcox. Simulation of Transition with a Two-Equation Turbulence Model. *AIAA Journal*, 32(2):247–255, 1994.
- [2] A. Hassan Eric, S. Warren Hassan. A Transition Closure Model for Predicting Transition. In *AIAA-1997-975502*, 1997.
- [3] Menter R. F. Langtry, R. B. Transition Modeling for General CFD Applications in Aeronautics. In *AIAA paper*, number 2005-522, 2005.
- [4] M. White Frank. *Viscous Fluid Flow*. McGraw Hill Science Engineering Math, 1991.
- [5] B. Thwaites. Approximate Calculation of the Laminar Boundary Layer. *Aeronaut. Q.*, 1:245–280, 1949.
- [6] Michel Kohler. Development and Implementation of a Method for Solving the Laminar Boundary Layer Equations in Airfoil Flows. Master’s thesis, Darmstadt University, 2011.
- [7] A. M. O. Smith and Gamberoni N. Transition Pressure Gradient and Stability Theory. Technical Report Rept. ES26388, Douglas Aircraft Co., EI Segundo, California, 1956.
- [8] J. L. Van Ingen. A suggested Semi-empirical Method for the Calculation of the Boundary Layer Transition Region. Technical Report Rept. UTH-74, University of Technology, Department of Aero. Eng., Delft, 1956.
- [9] R. Michel. Etude de la Transition sur les Profils d’Aile; Etablissement d’un Critere de Determination de Point de Transition et Calcul de la Trainee de Profile Incompressible, ". Technical report, ONERA, 1951.
- [10] Y. Lian and W. Shyy. Laminar-Turbulent Transition of a Low Reynolds Number Rigid or Flexible Airfoil. *AIAA*, 45:1501–1513, 2007.
- [11] M. T. Artur and C. J. Atkin. Transition Modeling for Viscous Flow Prediction. In *AIAA 2006-3052*, 2006.
- [12] S. A. McKeel. *Numerical Simulation of the Transition region in hypersonic Flow*. PhD thesis, Blacksburg, Virginia, 1996.
- [13] Harris J. E. Warren, E. S. and H. A. Hassan. Transition Model for High-Speed Flow. *AIAA Journal*, 33(8):1391–1397, 1995.
- [14] R. Schmidt and S. Patankar. Simulating Boundary Layer Transition with Low-Reynolds Number k-e Turbulence Models. *Journal of Turbomachinery*, 113:18–26, 1991.
- [15] C. Lam and K. Bremhorst. A Modified Form of the k-e Model for Predicting Wall Turbulence. *ASME Journal of Fluids Engineering*, 103:456–460, 1981.
- [16] D. Arnal. Laminar-Turbulent Transition Problems in Supersonic and Hypersonic Flows. Technical report, AGARD-FDP-VKI, Special course on Aerothermodynamics of Hypersonic Vehicles, 1988.
- [17] S. Dhawan and R. Narasimha. Some Properties of Boundary Layer Flow During Transition from Laminar to Turbulent Motion. *Journal of Fluid Mechanics*, 3:418–436, 1958.

- [18] E. R. Van Driest and C. B. Blumer. Boundary Layer Transition: Freestream Turbulence and Pressure Gradient Effects. *AIAA Jou*, 1:1303–1306, 1963.
- [19] Y. B. Suzen and P. G. Huang. An Intermittency Transport Equation for Modeling Flow Transition. In *AIAA 2000-0287*, 2000.
- [20] J. Steelant and E. Dick. Modeling of Bypass Transition with Conditioned Navier-Stokes Equations Coupled to an Intermittency Transport Equation. *International Journal for Numerical Methods in Fluids*, 23:193–220, 1996.
- [21] J. R. Cho and M. K. Chung. A k-e-v Equation Turbulence Model. *Journal of Fluid Mechanics*, 237:301–322, 1992.
- [22] P. G. Huang and G. Xiong. Transition and Turbulence Modeling of Low Pressure Turbine Flows. In *AIAA 98-0399*, Reno, 1998.
- [23] R. E. Mayle and A. Schulz. The Path to Predicting Bypass Transition. *Journal of Tur*, 119:405–411, 1997.
- [24] D. K. Walters and J. K. Leylek. A New Model for Boundary Layer Transition Using a Single-Point RANS Approach. *Journal of Tu*, 126:193–202, 2004.
- [25] Esch T. Menter, F. R. and S. Kubacki. Transition Modeling Based on Local Variables. In *Proceedings of the 5th International Symposium on Engineering Turbulence Modeling and Measurements, Elsevier, Amsterdam*, 2002.
- [26] Merci B. De Langhe C. Lodefier, K. and E. Dick. Intermittency Based RANS Bypass Transition Modeling. *Progress in Computational Fluid Dynamics*, 6:–, 2006.
- [27] J. Steelant and E. Dick. Modeling of Laminar-Turbulent Transition for High Freestream Turbulence. *Journal of Fluid Engineering*, 123:22–30, 2001.
- [28] S. Medida and J. Beader. Numerical Prediction of Static and Dynamic Stall Phenomena using the gamma-Rey Transition Model. In *American Helicopter Society 67th Annual Forum*, 2011.
- [29] Vinod K. Lakshminarayan Aniket, C. Aranake and Karthik Duraisamy. Assessment of Transition Model and CFD Methodology for Wind Turbine Flows. In *AIAA-2012-2720*, 2012.
- [30] A. M. Savill. Some Recent Progress in the Turbulence Modeling of by-pass Transition. *Near wall turbulent flow*, 1:829, 1993.
- [31] E. Chaput. Application-Oriented Synthesis os Work Presented in Chapter 2. *Notes on Numerical Fluid Mechanics*, 58:327–346, 1997.